Biomechanics and Modeling in Mechanobiology (2019) 18:57–68
https://doi.org/10.1007/s10237-018-1067-y

ORIGINAL PAPER

Effects of hydration and mineralization on the deformation mechanisms of collagen fibrils in bone at the nanoscale

Marco Fielder[1] · **Arun K. Nair**[1,2]

Received: 5 April 2018 / Accepted: 30 July 2018 / Published online: 7 August 2018

Abstract
Bone is a biomaterial with a structural load-bearing function. Investigating the biomechanics of bone at the nanoscale is important in application to tissue engineering, the development of bioinspired materials, and for characterizing factors such as age, trauma, or disease. At the nanoscale, bone is composed of fibrils that are primarily a composite of collagen, apatite crystals (mineral), and water. Though several studies have been done characterizing the mechanics of fibrils, the effects of variation and distribution of water and mineral content in fibril gap and overlap regions are unexplored. We investigate how the deformation mechanisms of collagen fibrils change as a function of mineral and water content. We use molecular dynamics to study the mechanics of collagen fibrils of 0 wt%, 20 wt%, and 40 wt% mineralization and 0 wt%, 2 wt%, and 4 wt% hydration under applied tensile stresses. We observe that the stress–strain behavior becomes more nonlinear with an increase in hydration, and an increase in mineral content for hydrated fibrils under tensile stress reduces the nonlinear stress versus strain behavior caused by hydration. The Young's modulus of both non-mineralized and mineralized fibrils decreases as the water content increases. As the water content increases, the gap/overlap ratio increases by approximately 40% for the non-mineralized cases and 16% for the highly mineralized cases. Our results indicate that variations in mineral and water content change the distribution of water in collagen fibrils and that the water distribution changes the deformation of gap and overlap regions under tensile loading.

Keywords Mineralization in bone · Mechanisms of deformation · Molecular modeling of bone · Collagen fibrils

1 Introduction

Bone is a composite biomaterial whose primary purpose is a load-bearing function (Fratzl 2008) and is composed of approximately 30% collagen protein, 60% hydroxyapatite mineral, and 10% water (Currey 2002; Dorozhkin and Epple 2002). Understanding the structure of bone is important for uncovering its material properties, which can change due to factors such as age, trauma, or diseases and conditions such as osteogenesis imperfecta or Ehlers–Danlos syndrome (Rauch and Glorieux 2004), and is also important in the development of novel materials inspired by bone's structure and material properties. Previous studies of bone at the nanoscale have used experimental methods, for example X-ray diffraction, to investigate the nanoscale structure of bone (Hang and Barber 2011; Samuel et al. 2016; Sasaki and Odajima 1996; Wells et al. 2015). Other studies use experimental methods such as atomic force microscopy (Pang et al. 2017; Uhlig and Magerle 2017; van der Rijt et al. 2006), micro-mechanical devices (Eppell et al. 2006; Minary-Jolandan and Yu 2009), or nuclear magnetic resonance (Gul-E-Noor et al. 2015) to study the nanoscale structure and elasticity of bone. Computational techniques are also used to study bone's nanoscale properties and include density functional theory and molecular dynamics (Depalle et al. 2016; Dubey and Tomar 2013; Gautieri et al. 2011; Nair et al. 2013; Streeter and de Leeuw 2010; Tang et al. 2010; Tourell and Momot 2016; Zhang et al. 2007). These studies primarily focus on dynamic changes in nanoscale bone structure, and what governs the interactions and deformation mechanisms of nanoscale bone. While these studies have investigated changes in mechanical properties due to the independent variations in mineral

✉ Arun K. Nair
nair@uark.edu

[1] Multiscale Materials Modeling Lab, Department of Mechanical Engineering, University of Arkansas, Fayetteville, AR, USA

[2] Institute for Nanoscience and Engineering, University of Arkansas, 731 W. Dickson Street, Fayetteville, AR, USA

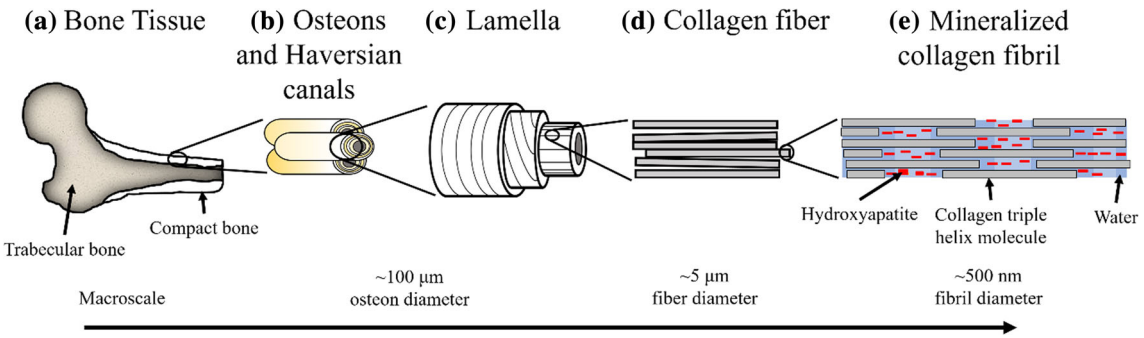

Fig. 1 Schematic representing the hierarchical structure of compact bone in descending order of length scales: **a** macroscale bone tissue, **b** micrometer scale compact bone composed of tightly packed and aligned tubular osteons. At the center of the osteons are haversian canals. An individual osteon is approximately 100 µm in diameter. **c** Single osteon composed of multiple concentric layers of lamella surrounding the haversian canal. **d** Lamella layer composed of tightly packed and aligned collagen fibers that are approximately 5 µm in diameter. An individual collagen fiber is composed of bundles of collagen fibrils that are approximately 500 nm in diameter. **e** Collagen fibril composed of a staggered arrangement of triple helix collagen protein molecules (gray), while apatite crystals (red) and water (blue) fill the gaps between collagen molecules

and water content, to date no study has been done to investigate how the simultaneous variation in mineral and water content changes the nanoscale mechanics of bone. Extensive work has also been done to investigate the properties of bone at the microscale using finite element method (Ahsan 2017; Lin et al. 2017; Liu et al. 2014; Thomopoulos et al. 2006). Finite element method remains an important computational tool to investigate the mechanical strength, and deformation and fracture behavior of bone, where the nanoscale properties predicted by atomistic methods can be an input to the microscale models.

Bone is hierarchical, with different structures at different size scales, which allows bone to be lightweight and tough (Currey 2002; Fratzl 2008; Gautieri et al. 2011). The hierarchical structure is represented in Fig. 1. At the macroscale, bone is composed of trabecular bone and cortical bone. Trabecular bone comprises mainly the interior of bone and has a porous and more random structure. Cortical bone, or compact bone, comprises mainly the exterior of bone and has a dense and ordered layer structure. At the millimeter scale, cortical bone consists of osteons and haversian canals that are composed of multiple concentric layers known as lamella that surround the haversian canals. The individual lamella is composed of densely packed collagen protein fibers at the low micrometer scale that align themselves in a single direction. The orientation of collagen fibers between lamella layers also varies, as represented in Fig. 1c. The collagen fibers in the lamella are composed of smaller bundles of collagen fibrils at the nanometer scale that are embedded in an extrafibrillar mineral matrix. Experiments show that the collagen fibrils are a composite of type I collagen, apatite crystals, and water (Currey 2002). The apatite has been shown to mineralize in the gaps between the collagen fibrils (Nudelman et al. 2010; Wang et al. 2012), and this mineralization between the collagen molecules in the fibril is known as intrafibrillar mineralization. Water in fibrils consists of mobile water located in the gap region and between collagen and apatite crystals, and structural water bound to collagen molecules and apatite crystals (Gul-E-Noor et al. 2015; Samuel et al. 2014; Zhang et al. 2007).

Previous experimental and computational studies did not focus on the variation of the intrafibrillar mineral and water content in fully 3D atomistic collagen fibrils and how this variation affects the mechanics of deformation at the nanoscale, especially in the gap and overlap regions. This is important because it is known that bone water content at the nanoscale is known to decrease due to increased mineralization (Bala and Seeman 2015; Nyman et al. 2006; Timmins and Wall 1977). Bone mineral and water content have also been shown to decrease with age (Mueller et al. 1966). Water is also known to be crucial in mediating the interactions within fibrils (Samuel et al. 2016).

The objective of this study is to quantify how the mechanical behavior and properties of collagen fibrils and its constituents at the nanoscale change as a function of both intrafibrillar mineral and water content due to an applied stress. We perform this study using molecular dynamics models of collagen fibrils. We investigate how the change in both mineral content and water content affects the mechanical behavior of collagen fibrils by performing tensile tests on models of fibrils with water contents of 0 wt%, ~2 wt%, and ~4 wt%, and degrees of intrafibrillar mineralization of 0 wt%, 20 wt%, and 40 wt%. We analyze the mechanical behavior of these fibrils through an analysis of the tensile stress versus linear strain behavior, Young's modulus, and observing the fibrils' deformation behavior.

2 Materials and methods

Type I collagen is the main component of bone fibrils and forms the matrix of the fibrils (Currey 2002). Another component of bone at the nanoscale is the mineral phase which is primarily apatite crystals in young and healthy bone. However, apatite can be subject to substitution to form other apatites, which can occur naturally, or be due to factors such as age, disease, or defect (Gul-E-Noor et al. 2015; Rauch and Glorieux 2004). We study here the nascent bone properties where the mineral phase is hydroxyapatite (HAP) with no substitutions (Nair et al. 2013), and which has the chemical composition of $Ca_{10}(PO_4)_6(OH)_2$. Non-collagenous proteins such as osteopontin and osteocalcin are also important for mediating the interaction between collagen and hydroxyapatite (Fantner et al. 2007; Poundarik et al. 2012). However, this mediation primarily takes place in the extrafibrillar matrix. Since our study investigates the intrafibrillar molecular interactions, the fibril model here only considers type I collagen which is the most abundant protein at the intrafibrillar level for nascent bone. Thus, the model presented here can be incorporated with non-collagenous proteins to study the mechanical properties of non-nascent bone. At the nanoscale, the mineralized collagen fibrils with type I collagen and HAP align along their longest length direction in a staggered periodic structure that creates what are known as gap and overlap regions, and a staggered periodicity length, known as the *D*-period, of approximately 67 nm (Fig. 2) (Orgel et al. 2006; Wess et al. 1995).

We develop computational models of three-dimensional collagen fibrils and simulate these models using the molecular dynamics package LAMMPS (Plimpton 1995). The models are developed with a structure based on the 3HR2 Protein Data Bank conformation (Orgel et al. 2006). The water and HAP mineral parameters for the MD fibril models are included in the Protein Structure Files and Protein Data Bank files and the extended CHARMM force field (MacKerell Jr et al. 1998). The water is defined by the TIP3P model in the CHARMM force field. Hydration of the fibrils was done using the hydration extension in the Visual Molecular Dynamics (VMD) program (Humphrey et al. 1996), where water molecules are distributed in the available voids in the fibril and allow us to study the effects of mobile water in collagen fibrils. For the non-mineralized fibrils, the water primarily locates in the gap regions, since they have the most available voids. For the mineralized fibrils, the water primarily locates in the overlap region voids, since the gap region voids are primarily occupied by hydroxyapatite. Since this study aims to investigate the mechanical behavior of collagen fibrils under reduced hydration conditions, hydration of the models was done between 0 wt% and 10 wt%. A hydration of 10 wt% agrees with previous studies of healthy bone water content (Currey 2002; Dorozhkin and Epple 2002; Hamed et al. 2010).

The unit cell for all models (Fig. 2) has a triclinic structure in agreement with experimental studies (Orgel et al. 2006; Wess et al. 1995). Studies of mineralized fibrils have shown that extrafibrillar mineralization can account for up to 75% of the total mineralization in bone (Beniash 2011; Bonar et al. 1985; Kinney et al. 2001; Lees et al. 1994; Nair et al. 2014). In this study, we only investigate the role of intrafibrillar mineralization on collagen fibril mechanical properties up to 40 wt% of the total fibrillar weight. The collagen fibril has the characteristic gap and overlap regions, a structure that has been experimentally determined (Gupta et al. 2006; Orgel et al. 2006) which agrees with the unit cell for the molecular dynamics fibril models studied here. The mineral is primarily present in the gap regions, which experiments show as the nucleation point of mineralization of collagen fibrils (Nudelman et al. 2010; Wang et al. 2012). We investigate three different percent volume values of mineralization: 0 wt%, 20 wt%, and 40 wt%. For each mineral percentage, we study three different degrees of water hydration: 0 wt%, ~2 wt%, and ~4 wt%. The representations of these models are visualized in Fig. 2 using VMD, to obtain a better visual of the structure of the fibrils at the various mineral and water contents. The respective water content for each model is also listed in Fig. 2. The ranges of tensile stresses we apply to the fibrils are 0.1 MPa (standard atmospheric pressure), 5 MPa, 8 MPa, and 20 MPa. The stress states are chosen in order to study the mechanical behavior of the collagen fibril models before the helical collagen molecules in the fibrils begin to fully uncoil due to the applied tensile load.

This study investigates the mechanical response of the fibrils in a quasi-static stress state and does not consider the fibril response as a function of the rate of applied stress. This is achieved by applying a known external pressure in the *x*-direction along the axis of the fibril to simulate the tensile testing of all models. Once the stress is applied, the fibril comes to an equilibrium conformation over the course of approximately 6 ns. The axes for the models are shown in Fig. 2i, and a visual showing the direction of applied stress is represented in Fig. 3a. All models are equilibrated in NPT ensemble at a temperature of 300 K, and the *y*- and *z*-directions are subject to 1 atm of pressure. The model also has periodic boundary conditions in all directions. After equilibration, all models are visualized in VMD to view its structure and deformation mechanisms. We confirm equilibration by plotting the root-mean-square distance (rmsd) between atoms versus simulation time. Equilibration is determined when the slope of the total rmsd between atoms versus time approaches zero, which happens for all models at approximately 6 ns. The average equilibrium unit cell length over the last 0.5 ns of the simulation is used, with its accompanying standard deviation, to compute the linear strain of

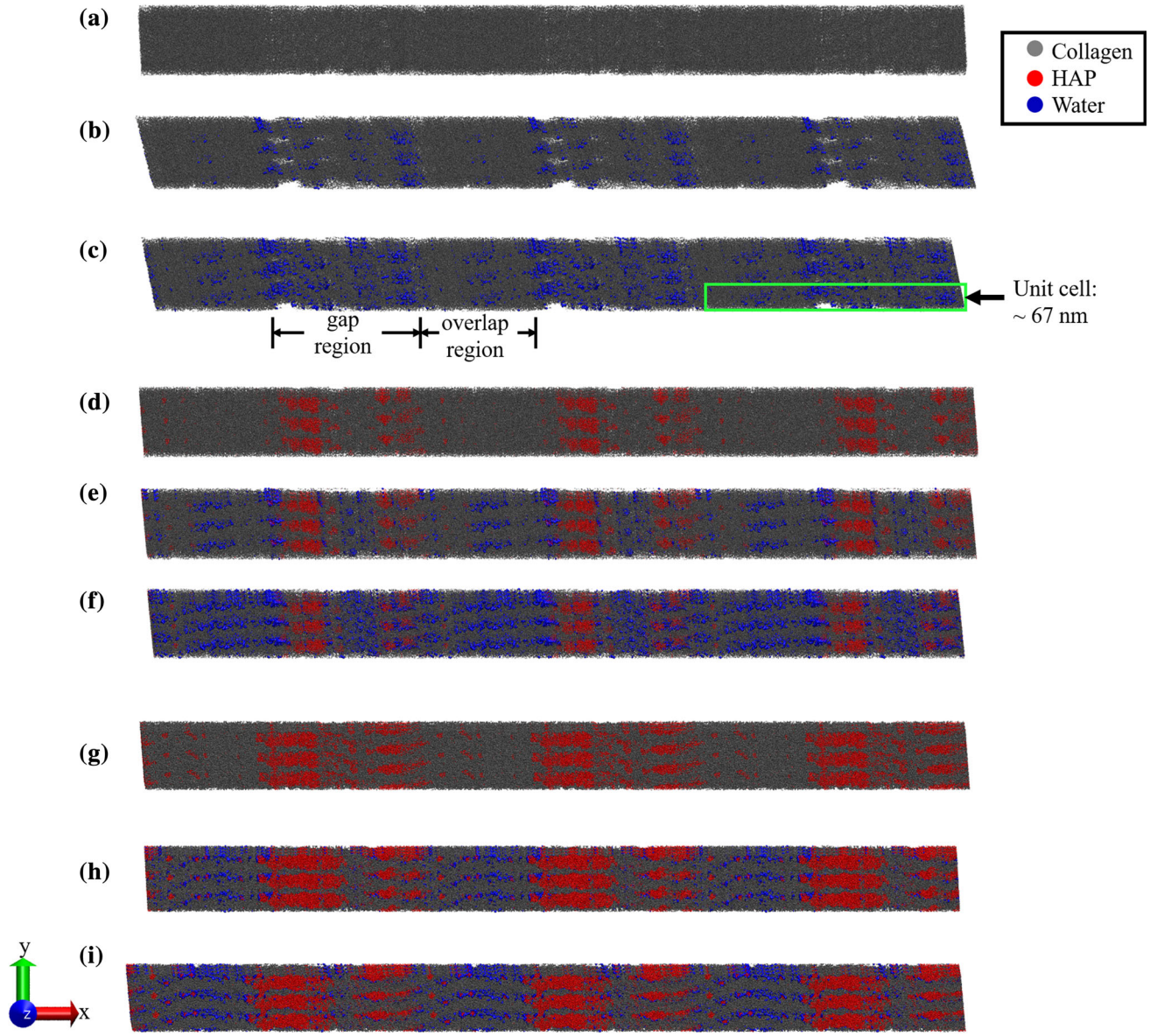

Fig. 2 Collagen fibrils with the varying mineral and water contents: **a** 0 wt% mineral and 0 wt% water. Also shown are the unit cell in green, and the gap and overlap regions. **b** 0 wt% mineral and 1.2 wt% water, **c** 0 wt% mineral and 3.2 wt% water, **d** 20 wt% mineral and 0 wt% water, **e** 20 wt% mineral and 1.4 wt% water, **f** 20 wt% mineral and 4.2 wt% water, **g** 40 wt% mineral and 0 wt% water, **h** 40 wt% mineral and 2.2 wt% water, **i** 40 wt% mineral and 3.3 wt% water. Water contents are approximated as 0 wt%, ~2 wt%, and ~4 wt%

the fibril. Linear strain along the fibril length is computed as $\varepsilon = \frac{l-l_o}{l_o}$, where l is the equilibrium unit cell length of the fibril model under external stress and l_o is the equilibrium unit cell length of the fibril model when it is subject to only 1 atm of pressure in all directions. The strain error bars are then determined by the rules governing the propagation of uncertainty (Bevington and Robinson 2003). We plot stress versus strain for all models and determine the Young's modulus from the slope of stress/strain curves, with the error bars again determined by the rules governing the propagation of uncertainty. We analyze the Young's modulus of all models versus the water content and finally perform an analysis of the deformation mechanisms in the collagen fibrils by observing the model equilibration over time and by analyzing the distance between terminal amino acid residues in the collagen molecules, which correspond to the lengths of the gap and overlap regions. We then use the ratio of gap length to overlap length to quantify how the gap and overlap regions deform with respect to one another. Similarly, the gap and overlap lengths in each simulation oscillate around an average value at equilibrium with a standard deviation, and the rules for the propagation of uncertainty are used to determine the error

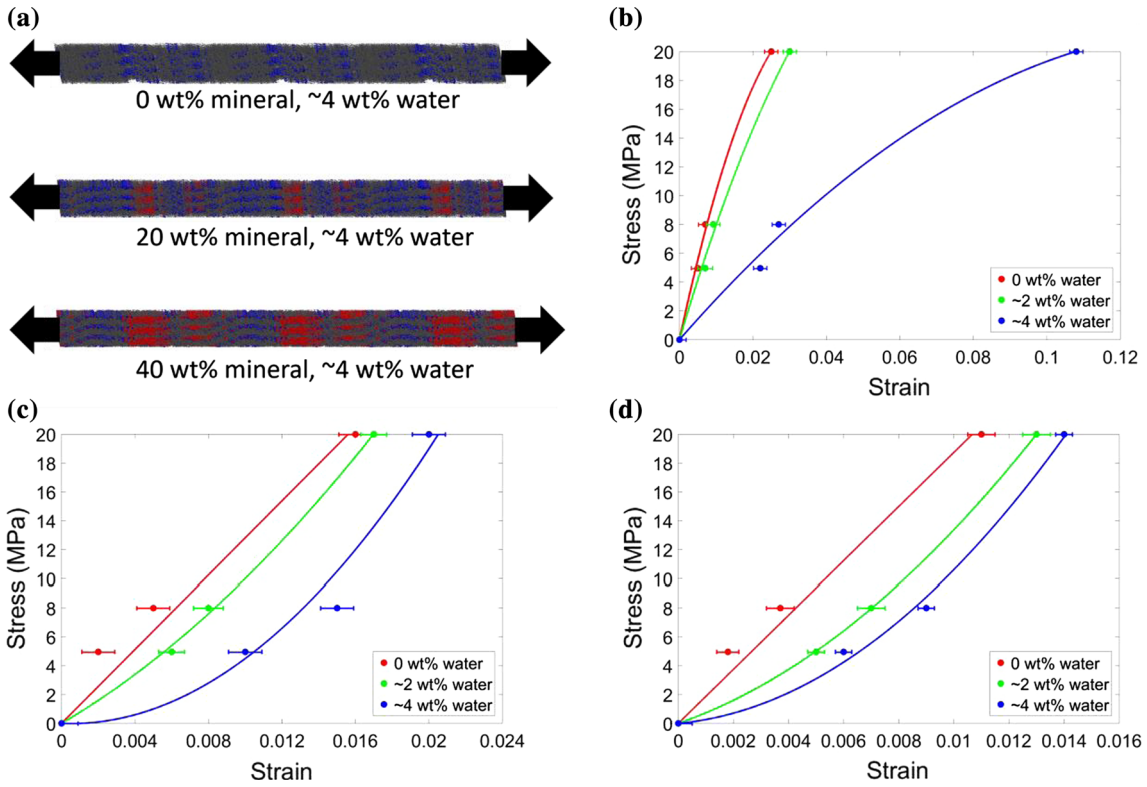

Fig. 3 **a** Diagram showing the tensile loading direction along the fibril length for hydrated fibrils of three different degrees of mineral content. Normal stress versus the linear strain of the fibrils is shown for models with mineral contents of **b** 0 wt%, **c** 20 wt%, **d** 40 wt%

bars of the gap/overlap ratio values. We perform a statistical analysis by determining a 95% confidence interval of the difference between the means for Young's modulus values and gap/overlap ratio values to determine the statistical significance (Bland and Altman 1986).

3 Results and discussion

From the stress–strain of non-mineralized fibril model (Fig. 3b), we observe an increase in water content from 0 to ~4 wt% results in an approximately 300% increase in strain for an applied tensile stress of 20 MPa. For the 20 wt% mineralization case, from Fig. 3c we observe increase in water content from 0 to ~4 wt% results in the stress versus strain behavior becoming more nonlinear, with an approximate 25% increase in deformation at a tensile stress of 20 MPa. The increase in strain at 20 MPa tensile stress for the 40 wt% mineralized fibril case, when comparing for water content of 0 wt% to ~4 wt%, is approximately 27%. For the 40 wt% mineralized fibril case, the total strain is reduced compared to the 20 wt% mineralized fibril at the same tensile stresses.

We observe that an increase in the fibril mineral content increases the stiffness of the fibril, while hydration causes the stiffness of the fibril to decrease, as shown in Fig. 3b–d. The results also indicate that hydration causes the stress versus strain behavior of the fibril to become more nonlinear, which agrees with experimental observations by Samuel et al. (2016) and Uhlig and Magerle (2017). We note, however, that the degree to which hydration reduces the modulus relative to the non-hydrated fibrils is minimized by the presence of mineral, which suggests that the mineral plays a dominating role in affecting the fibril modulus compared to water.

We compute the Young's modulus values for all cases and compare it with the change in the water content (Fig. 4). For the non-hydrated 0 wt% mineralized fibrils, the Young's modulus is $E \approx 1.2$ GPa. An increase in water content from 0 to ~2 wt% results in a ~33% decrease in Young's modulus. An increase in water content from ~2 to ~4 wt% results in a ~26% decrease in Young's modulus. For the non-hydrated 20 wt% mineralized fibrils in Fig. 4, $E \approx 1.3$ GPa. An increase in their water content from 0 to ~2 wt% results in a ~8% decrease in Young's modulus, while an increase in water content from 0 to ~4 wt% results in a ~15% decrease in Young's modulus. For the 40 wt% mineralized fibrils which are non-hydrated, the modulus is $E \approx 1.9$ GPa. An increase in water content from 0 to ~2 wt% results in a ~10% decrease in Young's modulus, as shown in Fig. 4. An increase in water

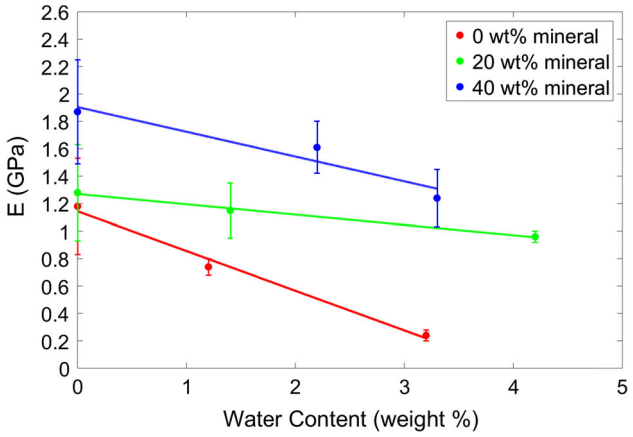

Fig. 4 Young's modulus (E) versus water content for three different degrees of fibril mineralization

content from 0 to ~4 wt% results in a ~15% decrease in Young's modulus. For all three degrees of mineralization, the decrease in the Young's modulus follows a linear trend as the fibril water content increases.

We observe that the Young's modulus of the 40 wt% mineralized fibrils is close to double the Young's modulus of the non-mineralized fibrils, regardless of water content. For example, at ~2 wt% water for the non-mineralized fibril and ~2 wt% water for the 40 wt% mineralized fibril, the Young's modulus of the non-mineralized fibril in Fig. 4 is 0.74 GPa, a difference of about 117% compared to 1.61 GPa for the 40 wt% mineralized fibril. We calculate a 95% confidence interval of the difference between the modulus values for fibrils with 0% mineral and 40% mineral at 0 wt% water and at ~4 wt% water. At 0 wt% water, we find the difference in modulus values to not be fully statistically significant, since we determined a 95% confidence interval (CI) of (−0.1381, 1.5181). However, at ~4 wt% water we find a statistically significant difference in their modulus values, with a 95% CI of the difference between the modulus values of (0.6573, 1.3427).

We also observe a linear trend for the decrease in the Young's modulus as the water content increases for all three degrees of fibril mineralization. The overall effect of hydration in reducing the Young's modulus of collagen fibrils is also observed in other studies on mineralized and non-mineralized collagen fibrils (Gautieri et al. 2011; Gul-E-Noor et al. 2015; Nair et al. 2014). A direct comparison with the Young's modulus values in our study in Fig. 4 agrees with previous studies of mechanical properties of collagen fibrils (Table 1), where both experimental and computational modeling methods were used to determine the Young's modulus of collagen fibrils. Experimental techniques use X-ray diffraction (Sasaki and Odajima 1996), atomic force microscopy (AFM) (van der Rijt et al. 2006), and micro-electromechanical system (MEMS) stretching (Eppell et al. 2006; Minary-Jolandan and Yu 2009), while the computa-

Table 1 Values for the Young's modulus obtained by other studies of collagen fibrils at various states of mineralization and hydration

Young's modulus (GPa)	Mineral and water content	Method of testing	References
0.43	0% mineral fully hydrated	X-ray diff.	(Sasaki and Odajima 1996)
0.2–0.8	0% mineral fully hydrated	AFM	(van der Rijt et al. 2006)
0.53	0% mineral fully hydrated	MEMS stretching	(Eppell et al. 2006)
1.1 in the gap region	0% mineral 0% water	MEMS stretching	(Minary-Jolandan and Yu 2009)
1.2 in the overlap region	0% mineral 0% water	MEMS stretching	(Minary-Jolandan and Yu 2009)
0.3–1.2	0% mineral fully hydrated	MD	(Gautieri et al. 2011)
1.8–2.25	0% mineral 0% water	MD	(Gautieri et al. 2011)
0.5–1.1	0% mineral 0% water	MD	(Nair et al. 2013)
1.3–2.7	20% mineral 0% water	MD	(Nair et al. 2013)
1.5–2.8	40% mineral 0% water	MD	(Nair et al. 2013)
1.96	42% mineral fully hydrated	Mathematical model	(Hamed et al. 2010)
2.4 ± 0.4	(46 ± 15)% mineral 13% water	AFM/SEM	(Hang and Barber 2011)

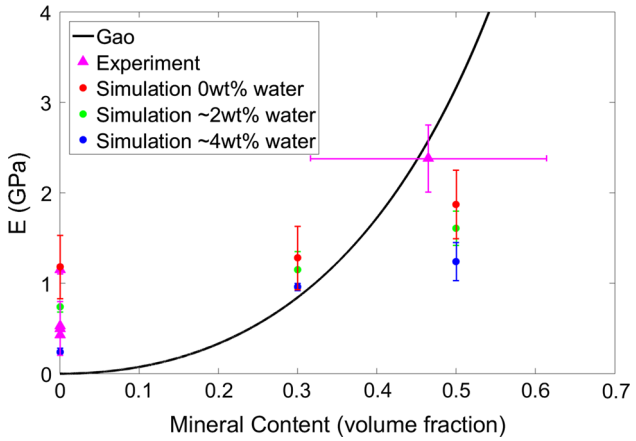

Fig. 5 Fibril Young's modulus (E) versus the fibril mineral content from this study and from experimental values in Table 1 compared to the effective modulus of mineralized fibrils determined by the Gao model

tional methods use molecular dynamics (MD) (Gautieri et al. 2011; Nair et al. 2013) and mathematical models (Hamed et al. 2010). Our study allows for the quantification of the change in fibril Young's modulus, when the fibril mineral and water content simultaneously vary. However, we find that for the mineralized fibrils, the decrease in modulus values caused by hydration is not statistically significant, although it is statistically significant for the non-mineralized fibrils. We determined a 95% CI for the difference between the maximum and minimum modulus values for each mineralization case in Fig. 4. For the fibrils with 0% mineral, the 95% CI was (0.3753, 1.5047). For the fibrils with 20% mineral, the 95% CI was (−0.2447, 0.8847). For the fibrils with 40% mineral, the 95% CI was (−0.066, 1.326). This supports the assertion that the presence of mineral minimizes water's effect on the fibril strain.

We also compare in Fig. 5 the Young's modulus values determined in this study to the effective modulus values determined by the Gao model (Gao et al. 2003). The Gao model formula is shown in Eq. 1 and was developed to calculate the effective modulus of mineralized collagen fibrils based on the mineralized collagen fibril model developed by Jäger and Fratzl (2000).

$$\frac{1}{\hat{E}} = \frac{4(1-\phi)}{G_{\mathrm{m}}\phi^2\rho^2} + \frac{1}{E_p\phi}. \tag{1}$$

In Eq. 1, the $\hat{E}$ is the effective modulus, ϕ is the mineral volume fraction, ρ is the mineral aspect ratio (~ 30) (Gao et al. 2003), G_{m} is the collagen shear modulus of 0.03 GPa (Yang et al. 2008), and E_p is the modulus of the mineral of 100 GPa (Gao et al. 2003). The experimental modulus values for non-mineralized fibrils in Fig. 5 are the experimental modulus values of non-mineralized fibrils in Table 1. The experimental value for the mineralized fibrils is from Hang and Barber et al. (2011) who determined modulus values of fibrils with mineral content varying from 32 to 61%. The modulus values determined in this MD study agree well within the error of that determined by the experiments.

At mineral volume fractions close to 0%, the modulus values in this study are higher than that determined by the Gao model. This is due to the mineral volume fraction term in Eq. 1, which causes the effective modulus to approach zero as the mineral volume fraction approaches zero. At mineral volume fractions of 0%, we find the results of this study agree most closely with the Gao model for fibrils with higher water content.

At mineral volume fractions of 50%, the modulus values from this study are lower than those determined by the Gao model. This is again due to the mineral volume fraction term in Eq. 1. The maximum value possible for ϕ is one. When ϕ approaches one, in Eq. 1 the effective modulus becomes approximately the modulus of mineral, which neglects the full effects of collagen protein and water on the elastic modulus of highly mineralized fibrils. At mineral volume fractions of 50%, we find the results of this study follow with the Gao model for fibrils with no water content. The modulus values in this study also agree with the Gao model at intermediate intrafibrillar mineral volume fractions of 30%.

We investigate the deformation mechanisms as both the mineral and water content changes in the fibrils. To obtain

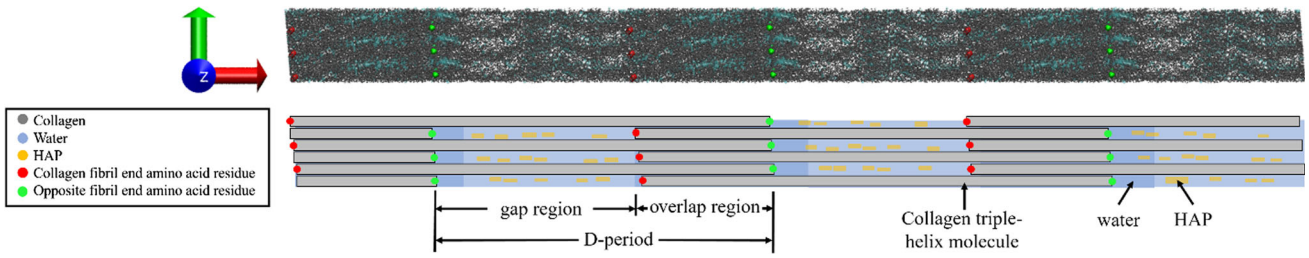

Fig. 6 A fully atomistic collagen fibril is visualized at the top of the figure. A schematic of the fibril is shown below. The collagen molecule end residues are represented in green and red color and show the end of the gap and overlap regions. Mineral is not included in the fully atomistic representation in order to better visualize the gap and overlap regions created by the collagen molecules

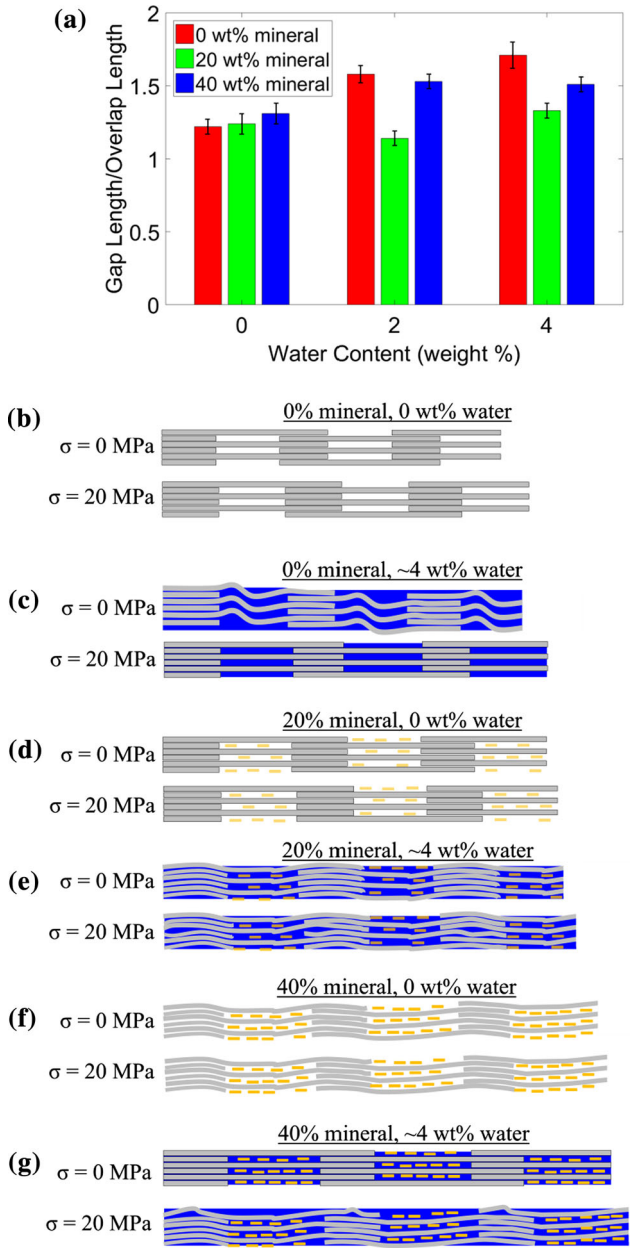

Fig. 7 **a** Average gap/overlap ratio for each fibril model. **b–g** Schematics of the lengthening and deformation of the fibril models are shown

the mechanics of gap and overlap deformation mechanics, we obtain the terminal amino acid residues at opposite ends of each individual collagen molecule in the fibril (see the red and green points in Fig. 6). We use the distance between these terminal residues to determine the linear strain for the gap and overlap regions for a tensile stress applied along the fibril length. The deformation behavior of the gap and overlap regions of the collagen fibril models are represented in Fig. 7, along with the corresponding schematic diagrams for each model. The schematic diagrams shown in Fig. 7b–g also represent their respective collagen fibrils at an applied stress of 20 MPa, in order to better represent the effects of hydration and mineralization on deformation of the gap and overlap regions due to the applied stress.

For all fibril cases considered here, we find that the gap/overlap ratio has a linear variation for an applied stress less than 20 MPa. We determine an average gap/overlap ratio at each stress state for each fibril simulation. The average gap/overlap ratios for all cases are shown in Fig. 7a.

For the fibril cases of 0 wt% mineralization, we observe that an initial increase in the fibril water content causes the gap length to deform more relative to the overlap region. However, we observe that an increase in the fibril mineralization minimizes the effect of hydration to increase the gap length for the same applied stress. Once stress is applied to the fibril, the gap region deforms much less in the mineralized fibrils compared to the gap region deformation of the non-mineralized fibrils, since the gap regions are stiffer in the mineralized fibrils with the presence of mineral in the gap regions.

The results in Fig. 7b, c demonstrate that, for the non-mineralized fibrils, hydration of the fibril causes the ratio of the gap length of the fibril and the overlap length of the fibril to increase under the same applied stress. This is due to the fact that, in the non-mineralized fibril case, approximately 80% of the water is located in the gap region where there is more space for the water molecules to occupy between the collagen molecules. We determine this from Figs. 2b and 7b, c, where the addition of water causes the gap region to deform more compared to the deformation of the overlap region at 20 MPa applied stress. Although the water is still located primarily in the gap region, as the water content of the non-mineralized fibril increases from ~2 to ~4 wt%, the water occupies the spaces in the gap region and a slight amount of water also begins to fill void spaces in the overlap region. This still results in an increased difference in the gap/overlap ratio, but to a lesser degree than the difference in gap/overlap ratio from a change in water content from 0 to ~2 wt%, which we observe from the results in Fig. 7a. The water distribution difference when comparing between ~2 and ~4 wt% is observed in Fig. 2b.

We also find that hydrating the non-mineralized fibril results in a slight folding of the collagen as can be seen comparing Fig. 7b, c. Since most of the water is located in the gap regions of the fibril, we observe most of this folding happening in the fibril gap regions. As stress is applied to the fibril, the fibril first undergoes straightening, before experiencing molecular stretching. A similar result for deformation mechanisms was observed by Andriotis et al. (2018) in experimental tensile pulling of hydrated non-mineralized collagen fibrils. Although Andriotis et al. observed an expansion in the spacing between collagen molecules, while we observe this expansion on a local level, we also observe that the overall spacing between collagen molecules decreases due to the

folding of the collagen. The intermolecular collagen spacing decreases by as much as 28% in the gap regions where we observed the most folding, compared to only an approximate 11% decrease in intermolecular collagen spacing in the overlap regions.

For the 20 wt% mineralized fibrils, the mineral is primarily in the gap region and causes strain in the gap region to decrease by 50%, even with changes in fibril water content from 0, to ~ 2 wt%, to ~ 4 wt%. The presence of mineral also reduces the effect of hydration on the gap/overlap ratio, where the addition of water does not cause as large of a magnitude change in the gap/overlap ratio in the 20 wt% mineralized fibrils as it does in the non-mineralized fibril, which is observed by a comparison of the 0 wt% mineral cases with the 20 wt% mineral cases in Fig. 7a.

The hydration of the 20 wt% mineralized fibrils to ~ 2 wt% water causes the gap/overlap ratio of the fibril to initially decrease, but then the gap/overlap ratio increases once the fibril water content increases to ~ 4 wt%. This is due to the fact that, in the 20 wt% mineralized fibrils, the mineral is primarily in the gap region, which results in the gap region having fewer spaces for the water to fill than the overlap region. Because of this, we find that the water is displaced to occupy the voids in the overlap region when the water content is ~ 2 wt% and causes the overlap region to expand and deform more relative to the overlap region of the non-hydrated fibril as stress is applied, while the deformation of the gap region remains relatively the same when comparing between the 0 and ~ 2 wt% hydrated fibrils at 20 wt% mineralization. However, as the water content increases to ~ 4 wt%, we find that the water occupies the remaining void spaces in both the gap and overlap regions, and the water becomes much more equally distributed throughout the fibril.

Approximately 60% of the water is in the gap regions, which we can also observe from Fig. 2e, f, where the more equal distribution of water in the fibril causes the gap region to also expand and deform more relative to the deformation of the gap region of the corresponding non-hydrated fibril as we apply more stress, thus increasing the gap/overlap ratio, as shown in Fig. 7a. Even though 60% of the water is in the gap regions, we find that the mineral in the gap regions inhibits the fibril from expanding in the direction perpendicular to the fibril length when the hydration increases. We determine that the intermolecular collagen spacing in the overlap regions expands by as much as 88% due to hydration, while the gap region intermolecular collagen spacing decreases by approximately 18%. This agrees with the observations by Andriotis et al. (2018), who observed an overall increase in intermolecular collagen spacing in non-mineralized fibrils. The mineral in the fibrils in our study prevents the fibril from folding and allows the hydration induced expansion to occur. Our results also additionally show how the change in intermolecular collagen spacing differs between the gap and overlap regions and how it is affected by intrafibrillar mineralization.

We also find that the fibril deformation mechanisms change as the fibril water content increases due to the change in water distribution. In the non-hydrated fibrils with 20% mineral, the primary deformation mechanism was stretching, observed through elongation of the collagen molecules. However, when hydrated, the primary deformation mechanisms were unfolding and the beginning of intermolecular sliding. This is shown in Fig. 7d, e. Unfolding is observed by the slight straightening of the overlap regions, which had folded due to the presence of water and lack of mineral to prevent folding. The initiation of sliding is observed by the separation of collagen molecules adsorbed to one another and occurs primarily in the overlap regions where mineral does not assist as much in holding collagen molecules together.

For the 40 wt% mineralized fibril, the hydration of the fibril causes the gap/overlap ratio of the fibril to increase, as shown in Fig. 7a. In the 40 wt% mineralized fibril, the higher amount of mineralization causes a large degree of mineralization in the overlap region compared to 20 wt%, although a significant amount of mineral in the fibril is in the gap region. Such a large degree of mineral in both the gap and overlap regions allows the water to distribute itself uniformly throughout the fibril into the spaces in both the gap region and the overlap region. We find that approximately 47% of the water is in the gap regions, with the other 53% in the overlap regions. This causes the gap region of the 40 wt% mineralized fibril to deform more compared to the gap region deformation of the non-hydrated fibril of 40 wt% mineral when both experience the same applied stress.

For the 40 wt% mineralized fibril, at a water content of ~ 2 wt% most of the void spaces in the fibril are already filled by the water. As the water content of the 40 wt% mineralized fibril increases to ~ 4 wt%, the water fills the remaining void spaces in the fibril and the gap/overlap ratio increases. The presence of mineral in the gap regions resists the expansion of the gap region perpendicular to the fibril length. This leaves the gap region to expand primarily in the direction parallel to the fibril length, while the overlap regions do not expand as much as the gap regions in the direction parallel to the fibril length since they are free to expand perpendicular to the fibril length. This is evident when comparing the ~ 2 wt% water model to the ~ 4 wt% water model in Fig. 7a, where there is a minimal difference between their respective gap/overlap ratios. The small difference in the water distribution when comparing the ~ 2 wt% and ~ 4 wt% hydrated fibril with 40 wt% mineral is observed in Fig. 2h, i. To validate this, we compute the change in the perpendicular intermolecular collagen spacing due to hydration and determine the overlap regions expand by as much as 73%, while the gap regions only expand by as much as 13%.

As mentioned previously, we observe that as a higher tensile stress is applied to the fibril, the relation between the gap region deformation and the overlap region deformation remains approximately constant, regardless of the fibril water content. These results agree with the experimental work by Samuel et al. (2016), who observed a linear relation in bone between the mineral phase strain and the collagen phase strain, which from our observations corresponds primarily to the fibril gap regions and the fibril overlap regions, respectively. We find that the presence of water results in the initiation of molecular sliding and unfolding, which contrasts to more molecular stretching observed when no water is present in the fibril. However, the presence of mineral reduces the dissociation between collagen molecules caused by the presence of water, since the mineral resists the intermolecular sliding. This explains why in mineralized fibrils the unfolding and initiation of intermolecular sliding are primarily observed in the overlap regions, which have less mineral.

In determining a 95% CI of the difference between gap/overlap values, we find there is a statistically significant difference in gap/overlap ratios when comparing the 0% mineralized fibrils with the 20% mineralized fibrils, with a 95% CI of (0.1799, 0.3401). We find a statistically significant difference in the gap/overlap ratios when comparing the 20% mineralized fibrils with the 40% mineralized fibrils, with a 95% CI of (0.142, 0.278). We do not find there is a statistically significant difference in gap/overlap ratios when comparing the 0% mineralized fibrils with the 40% mineralized fibrils, with a 95% CI of (−0.0301, 0.1301). This suggests that as the intrafibrillar mineral content reduces from a high value (40%) to a low value (0%), there is a significant change in the gap and overlap region behavior at intermediate mineral contents (20%). Our results also allow us to use the fibril gap/overlap length ratio to quantify the changes in the linear deformation relation between the mineral and collagen phases of protein when the fibril mineral content and water content simultaneously vary.

4 Conclusions

We investigate the effect of water and mineral content of collagen fibrils on their mechanical behavior and properties such as stress versus strain behavior, Young's modulus, and comparisons of fibril gap and overlap region deformation behavior. The method of investigating these fibril properties is by a uniaxial tensile test along the fibril length using molecular dynamics method. This study finds the tensile Young's modulus of the 40 wt% mineralized fibrils is almost double the difference in the tensile Young's modulus of the 0 wt% mineralized fibrils, irrespective of the water content. We find that as the degree of mineralization of the fibril increases, the effect of water to change the magnitude of deformation of the gap and overlap regions decreases, although this effect is more pronounced in the gap region where the mineral first nucleates.

For non-mineralized fibrils, water first fills the void spaces in the gap regions and only begins to fill the void spaces in overlap region as the water content of the fibril increases to around ~4 wt%. For the mineralized fibrils, water primarily occupies the void spaces in the overlap regions at low water contents, before filling the void spaces in the gap regions and distributing more evenly throughout the whole fibril as the water content of the fibril increases to around ~4 wt%.

A hydration of up to ~4 wt% for the mineralized fibrils allows the water to become distributed also in the gap region, which allows the gap region to be able to deform more. Thus, the gap/overlap ratio increases as the overlap region expands transversely and the gap region expands longitudinally. This is explained by the higher stiffness of the mineralized gap region, which a previous study has shown takes up the largest amount of stress in the whole fibril (Nair et al. 2013). This means that a large degree of hydration of the mineralized fibrils is needed to allow the gap region that is taking up the largest amount of total fibril stress to be able to deform more. A degree of hydration of a mineralized fibril that is too low, near ~2 wt%, will only allow the overlap region to deform more, since water fills primarily the void spaces in the overlap region. This means that a reduction in fibril hydration can cause the mineralized gap regions to become stiffer and resist deformation, even if the water content of the fibril is high enough that the overlap regions remain hydrated and be able to deform more. The results of the current study on the distribution of water in collagen fibrils between the gap region and overlap region are useful for understanding how bone's nanoscale mechanical behavior changes when the bone mineral and water content changes. The results also have potential for use in the design of novel tissue engineering composites whose mechanical properties change as the scaffold mineral or water content changes as the scaffold either degrades or as in vivo environmental conditions change.

Acknowledgements MF and AKN would like to thank the support from Department of Mechanical Engineering, University of Arkansas, and also the Arkansas High Performance Computing Center (AHPCC). Authors also acknowledge the support in part by the National Science Foundation (NSF) under the Grants ARI#0963249, MRI#0959124, and EPS#0918970, and a grant from Arkansas Science and Technology Authority, managed by Arkansas High Performance Computing Center. We also acknowledge partial support from NSF Grant IIA 1457888.

Compliance with ethical standards

Conflict of interest Authors declare no conflict of interest.

References

Ahsan AS (2017) Effect of intrafibrillar mineralization on the mechanical properties of osteogenesisimperfecta bone using a cohesive finite element approach. The University of Texas, SanAntonio

Andriotis OG, Desissaire S, Thurner PJ (2018) Collagen Fibrils: Nature's Highly Tunable Nonlinear Springs. ACS nano 12:3671–3680

Bala Y, Seeman E (2015) Bone's Material Constituents and their Contribution to Bone Strength in Health, Disease, and Treatment. Calcif Tissue Int 97:308–326

Beniash E (2011) Biominerals-hierarchical nanocomposites: the example of bone. Wires Nanomed Nanobiotechnol 3:47–69

Bevington P, Robinson DK (2003) Data reduction and error analysis for the physical sciences. McGraw-Hill Education

Bland JM, Altman DG (1986) Statistical methods for assessing agreement between two methods of clinical measurement. Lancet 1:307–310

Bonar LC, Lees S, Mook HA (1985) Neutron-Diffraction Studies of Collagen in Fully Mineralized Bone. J Mol Biol 181:265–270

Currey JD (2002) Bones: structure and mechanics. Princeton University Press, Princeton

Depalle B, Qin Z, Shefelbine SJ, Buehler MJ (2016) Large deformation mechanisms, plasticity, and failure of an individual collagen fibril with different mineral content. J Bone Miner Res 31:380–390

Dorozhkin SV, Epple M (2002) Biological and medical significance of calcium phosphates. Angew Chem Int Ed 41:3130–3146

Dubey DK, Tomar V (2013) Ab initio investigation of strain dependent atomistic interactions at two tropocollagen-hydroxyapatite interfaces. J Eng Mater Technol 135:021015

Eppell S, Smith B, Kahn H, Ballarini R (2006) Nano measurements with micro-devices: mechanical properties of hydrated collagen fibrils. J R Soc Interface 3:117–121

Fantner GE, Adams J, Turner P, Thurner PJ, Fisher LW, Hansma PK (2007) Nanoscale ion mediated networks in bone: osteopontin can repeatedly dissipate large amounts of energy. Nano Lett 7:2491–2498

Fratzl P (ed) (2008) Collagen: structure and mechanics, an introduction. In: Collagen. Springer, Boston, pp 1–13

Gao H, Ji B, Jäger IL, Arzt E, Fratzl P (2003) Materials become insensitive to flaws at nanoscale: lessons from nature. Proc Natl Acad Sci 100:5597–5600

Gautieri A, Vesentini S, Redaelli A, Buehler MJ (2011) Hierarchical structure and nanomechanics of collagen microfibrils from the atomistic scale up. Nano Lett 11:757–766

Gul-E-Noor F, Singh C, Papaioannou A, Sinha N, Boutis GS (2015) Behavior of water in collagen and hydroxyapatite sites of cortical bone: fracture, mechanical wear, and load bearing studies. J Phys Chem C 119:21528–21537

Gupta HS, Seto J, Wagermaier W, Zaslansky P, Boesecke P, Fratzl P (2006) Cooperative deformation of mineral and collagen in bone at the nanoscale. P Natl Acad Sci USA 103:17741–17746

Hamed E, Lee Y, Jasiuk I (2010) Multiscale modeling of elastic properties of cortical bone. Acta Mech 213:131–154

Hang F, Barber AH (2011) Nano-mechanical properties of individual mineralized collagen fibrils from bone tissue. J R Soc Interface 8:500–505

Humphrey W, Dalke A, Schulten K (1996) VMD: visual molecular dynamics. J Mol Graph 14:33–38

Jäger I, Fratzl P (2000) Mineralized collagen fibrils: a mechanical model with a staggered arrangement of mineral particles. Biophys J 79:1737–1746

Kinney JH, Pople JA, Driessen CKH, Breunig TM, Marshall GW, Marshall SJ (2001) Intrafibrillar mineral may be absent in dentinogenesis imperfecta type II (DI-II). J Dent Res 80:1555–1559

Lees S, Prostak KS, Ingle VK, Kjoller K (1994) The loci of mineral in turkey leg tendon as seen by atomic-force microscope and electron-microscopy. Calcif Tissue Int 55:180–189

Lin L, Samuel J, Zeng X, Wang X (2017) Contribution of extrafibrillar matrix to the mechanical behavior of bone using a novel cohesive finite element model. J Mech Behav Biomed 65:224–235

Liu Y, Thomopoulos S, Chen C, Birman V, Buehler MJ, Genin GM (2014) Modelling the mechanics of partially mineralized collagen fibrils, fibres and tissue. J R Soc Interface 11:20130835

MacKerell AD Jr, Bashford D, Bellott M, Dunbrack RL Jr, Evanseck JD, Field MJ, Fischer S, Gao J, Guo H, Ha S (1998) All-atom empirical potential for molecular modeling and dynamics studies of proteins. J Phys Chem B 102:3586–3616

Minary-Jolandan M, Yu M-F (2009) Nanomechanical heterogeneity in the gap and overlap regions of type I collagen fibrils with implications for bone heterogeneity. Biomacromolecules 10:2565–2570

Mueller KH, Trias A, Ray RD (1966) Bone density and composition: age-related and pathological changes in water and mineral content. JBJS 48:140–148

Nair AK, Gautieri A, Chang S-W, Buehler MJ (2013) Molecular mechanics of mineralized collagen fibrils in bone. Nat Commun 4:1724

Nair AK, Gautieri A, Buehler MJ (2014) Role of intrafibrillar collagen mineralization in defining the compressive properties of nascent bone. Biomacromolecules 15:2494–2500

Nudelman F, Pieterse K, George A, Bomans PHH, Friedrich H, Brylka LJ, Hilbers PAJ, de With G, Sommerdijk NAJM (2010) The role of collagen in bone apatite formation in the presence of hydroxyapatite nucleation inhibitors. Nat Mater 9:1004–1009

Nyman JS, Roy A, Shen XM, Acuna RL, Tyler JH, Wang XD (2006) The influence of water removal on the strength and toughness of cortical bone. J Biomech 39:931–938

Orgel JPRO, Irving TC, Miller A, Wess TJ (2006) Microfibrillar structure of type I collagen in situ. P Natl Acad Sci USA 103:9001–9005

Pang X, Lin L, Tang B (2017) Unraveling the role of calcium ions in the mechanical properties of individual collagen fibrils. Sci Rep 7:46042

Plimpton S (1995) Fast parallel algorithms for short-range molecular-dynamics. J Comput Phys 117:1–19

Poundarik AA, Diab T, Sroga GE, Ural A, Boskey AL, Gundberg CM, Vashishth D (2012) Dilatational band formation in bone. Proc Natl Acad Sci 109:19178–19183

Rauch F, Glorieux FH (2004) Osteogenesis imperfecta. Lancet 363:1377–1385

Samuel J, Sinha D, Zhao JC-G, Wang X (2014) Water residing in small ultrastructural spaces plays a critical role in the mechanical behavior of bone. Bone 59:199–206

Samuel J, Park J-S, Almer J, Wang X (2016) Effect of water on nanomechanics of bone is different between tension and compression. J Mech Behav Biomed Mater 57:128–138

Sasaki N, Odajima S (1996) Elongation mechanism of collagen fibrils and force–strain relations of tendon at each level of structural hierarchy. J Biomech 29:1131–1136

Streeter I, de Leeuw NH (2010) Atomistic modeling of collagen proteins in their fibrillar environment. J Phys Chem B 114:13263–13270

Tang Y, Ballarini R, Buehler MJ, Eppell SJ (2010) Deformation micromechanisms of collagen fibrils under uniaxial tension. J R Soc Interface 7:839–850

Thomopoulos S, Marquez JP, Weinberger B, Birman V, Genin GM (2006) Collagen fiber orientation at the tendon to bone insertion and its influence on stress concentrations. J Biomech 39:1842–1851

Timmins PA, Wall JC (1977) Bone water. Calcif Tissue Res 23:1–5

Tourell MC, Momot KI (2016) Molecular dynamics of a hydrated collagen peptide: insights into rotational motion and residence times of single-water bridges in collagen. J Phys Chem B 120:12432–12443

Uhlig MR, Magerle R (2017) Unraveling capillary interaction and viscoelastic response in atomic force microscopy of hydrated collagen fibrils. Nanoscale 9:1244–1256

van der Rijt JA, van der Werf KO, Bennink ML, Dijkstra PJ, Feijen J (2006) Micromechanical testing of individual collagen fibrils. Macromol Biosci 6:697–702

Wang Y, Azais T, Robin M, Vallee A, Catania C, Legriel P, Pehau-Arnaudet G, Babonneau F, Giraud-Guille MM, Nassif N (2012) The predominant role of collagen in the nucleation, growth, structure and orientation of bone apatite. Nat Mater 11:724–733

Wells HC, Sizeland KH, Kayed HR, Kirby N, Hawley A, Mudie ST, Haverkamp RG (2015) Poisson's ratio of collagen fibrils measured by small angle X-ray scattering of strained bovine pericardium. J Appl Phys 117:044701

Wess TJ, Hammersley A, Wess L, Miller A (1995) Type-I collagen packing, conformation of the triclinic unit-cell. J Mol Biol 248:487–493

Yang L, Fitie CF, van der Werf KO, Bennink ML, Dijkstra PJ, Feijen J (2008) Mechanical properties of single electrospun collagen type I fibers. Biomaterials 29:955–962

Zhang DJ, Chippada U, Jordan K (2007) Effect of the structural water on the mechanical properties of collagen-like microfibrils: a molecular dynamics study. Ann Biomed Eng 35:1216–1230